Notable Behaviours of Liquid Draining in a Tank with a Bluff-Body as an Air-Core Suppression Mechanism

Fadhilah Mohd Sakri[1,*], Mohamed Sukri Mat Ali[2], Ivanov Konstantin Georgievich[3], Nurshafinaz Mohd Maruai[2], Ahmad Faiz Mohammad[2]

1   Department of Aerospace, Universiti Kuala Lumpur–Malaysia Institute of Aviation Technology (UniKL MIAT), 43800 Dengkil, Malaysia
2   Wind Engineering Laboratory, Malaysia-Japan International Institute of Technology, UTM Kuala Lumpur, 54100, Kuala Lumpur, Malaysia
3   Faculty of Physics, Saint Petersburg State University of Industrial Technologies and Design, Saint Petersburg, Russia

ARTICLE INFO	ABSTRACT
	The air-core vortex that generally shows up as fluid channels inside a tank lessens the channel rate, which can decrease the fluid supply's depleting proficiency and life expectancy. This paper examines the fundamental measures for passively controlling the presence of such an air-core. OpenFOAM was used to examine the effects of a disc plate and a cone on the formation of an air-core vortex within a liquid draining tank. The research revealed various drainage behaviours. In the case of the disc plate, the draining process displayed three distinct stages: the normal regime, transitional regime, and air-core regime. However, when the disc was substituted with a cone, only one behaviour corresponding to the air-core regime was evident. At the point of liquid passing the disc plate or cone, the air-core vortex emerged. For the disc plate scenario, a partial vortex ring was observed whereas for the cone plate, no vortex ring was perceived.

1. Introduction

The efficiency of liquid drainage from tanks is hindered by the formation of an air-core vortex, and the underlying physical mechanisms of this phenomenon remain incompletely understood [1]. As indicated by Basu *et al.,* [2], the air-core vortex involves the rotational motion of liquid with entrained air through the vortex core [3]. Initiated by the formation of a dip in the liquid surface, this dip transforms into an air-core once it reaches the drain outlet at the critical height, H_c, significantly diminishing drainage efficiency. The dip evolves into an air-core vortex, generating a lengthy, slender string shape that extends to the tank bottom [4]. The rotational flow intensifies as the fluid drains, reinforcing the air-core vortex [2]. When the vortex core reaches the tank bottom, the drain rate decreases, and the outlet nozzle flow becomes unsteady and rotational. Numerous studies have endeavored to tackle this issue [5-6].

In recent years, various attempts [7-14] have been made to mitigate air-core vortex formation. Uki *et al.,* [15] developed a vortex breaker in a Gas-Liquid Separator, while Mahyari *et al.,* [16]

---

proposed a circular disc with blades and a porous wall as a vortex breaker for reducing the critical height in the liquid propellant of launch vehicles. Abramson *et al.,* [17] and Kinefuchi *et al.,* [18] found that the impact of the air-core vortex on flow rate can be nullified by installing a simple cross-type baffle over the orifice. Sohn *et al.,* [19] utilize d a vane-type suppressor and investigated the efficacy of an eccentric drain outlet [20] and a square cross-section [21] in suppressing vortices. However, these passive air-core control mechanisms have limitations, with the primary drawback being their inability to completely suppress air-core vortex formation.

To date, there are few studies that has investigated on behaviours of liquid draining in a tank with the existence of bluff-body as an air-core suppression mechanism. In light of this challenge, the aim of this research is to effectively employ the bluff-body shapes of a disc plate and a cone as a suppressor utilizing numerical methods. The liquid draining behaviours and flow visualization for both cases are compared.

2. Methodology
2.1 Numerical Procedure

The equations describing the conservation of mass and momentum for flows that are incompressible, transient, and involve free surfaces are provided below [4,22-24]:

$$\nabla.U = 0 \tag{1}$$

$$\frac{\partial \rho U}{\partial t} + \nabla.\rho UU - \nabla.(\rho \Gamma_U \nabla_U) = S_U(U) + g + F \tag{2}$$

where U is the instantaneous local velocity, ρ is the density, Γ is the diffusion coefficient, S represents all source terms, g is the gravitational acceleration and F is the force of volumetric surface tension. The Smagorinsky Large-Eddy Simulation is employed for computing smaller eddies [25]. The OpenFOAM open-source CFD package was used for simulating the fluid dynamics. The temporal term is discretised using the first-order scheme and the convection term is discretised using the total-variation diminishing scheme.

2.2 Test Case Description

Figure 1 displays the simulation configuration for the disc suppressor. In the initial segment, the disc plate is defined by a diameter of of $3d$ and a width of $0.5d$. Seven mounting heights, specifically $0.25d, 0.5d, 0.75d, d, 2d, 3d$ and $4d$ are examined to assess the sensitivity of gap distance in relation to flow parameters. The subsequent section will elaborate on the determination of the optimal height $H = d$ for the disc suppressor, leading to effective air-core suppression.

In the following segment, the disc suppressor is replaced with a cone of varying diameters to analyze the influence of cone geometry on the draining flow. The installation height is held constant at the previously determined optimal height $H = d$ from the disc simulation. Figure 2 depicts the simulation setup for the cone suppressor. To create more space near the outlet for liquid drainage, the cone is inverted, with the expectation that this configuration would improve the mass flow rate and discharge coefficient. Three distinct cone diameters $2d, 3d$ and $4d$ are simulated while maintaining a width of $0.5d$ and an installation height of $H = d$.
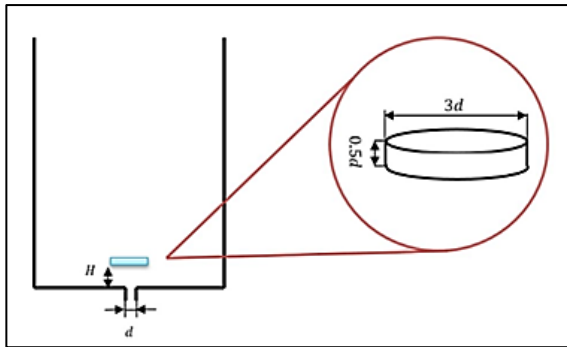
Fig. 1. Simulation setup for the disc suppressor
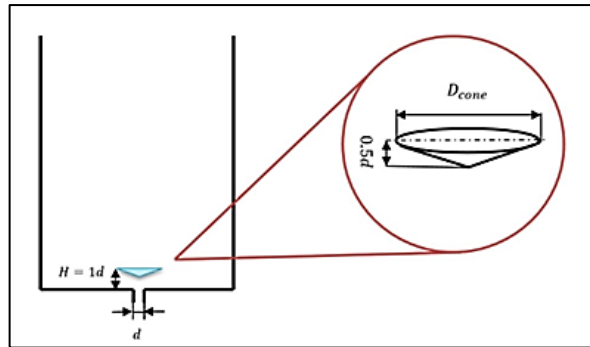
Fig. 2. Simulation setup for the cone suppressor

3. Results and Discussion

3.1 Draining Process

3.1.1 Disc simulation

As previously noted, three distinct draining behaviour regimes emerge in the case of the disc suppressor. The specific features of each regime are outlined below.

3.1.1.1 Normal draining

Figure 3 displays the liquid fraction near the outlet at installation heights of $0.25d, 0.5d$ and $0.75d$. In contrast to the baseline case (absent an air-core suppression mechanism) where the liquid fraction varies with draining time, the fraction remains constant until the completion of the draining process when a disc suppressor is employed at these installation heights. This observation implies the absence of air-core formation during the drainage when a disc suppressor is positioned at these specific heights.
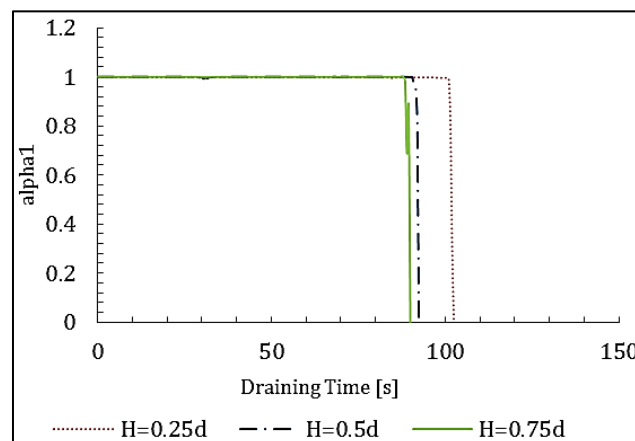
Fig. 3. Liquid fraction for installation heights of 0.25d, 0.5d, and 0.75d during the normal drainage regime

3.1.1.2 Transition

When the installation height is elevated to $H = d$, the liquid fraction ceases to remain constant and initiates oscillations at $t \geq 40$s (refer to Figure 4). Although the presence of an air-core vortex is not observed in this scenario, a thorough examination of the outcomes in Figure 5 reveals that external air bubbles are drawn upwards into the outlet due to the expansion of the low-pressure

region beneath the disc suppressor (refer to Figure 6 for comparison). Consequently, the pressure differential between the interior and exterior of the outlet induces the appearance of air bubbles. Nevertheless, the drainage process remains uninterrupted, with the presence of this practically negligible amount of air bubbles having no significant impact.
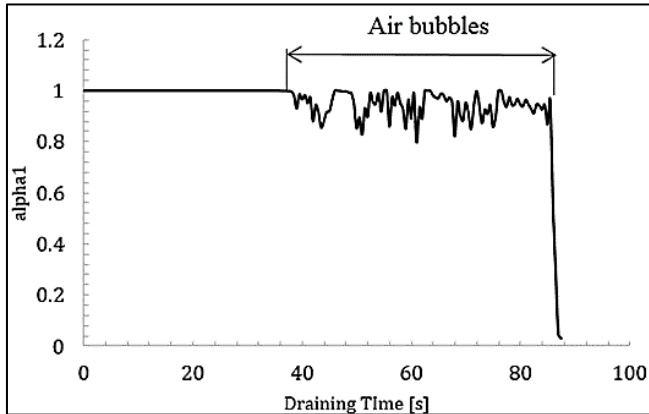
Fig. 4. Liquid fraction at the outlet with an installation height of $H = d$ during the transitional drainage regime
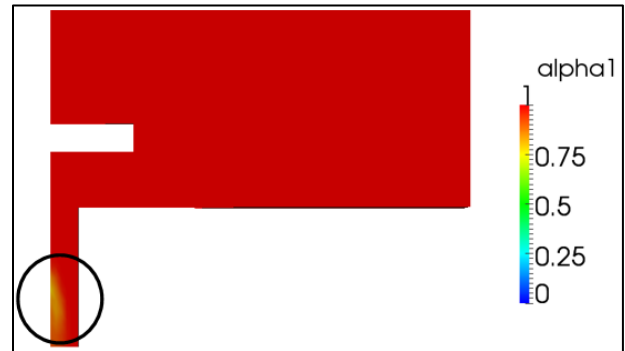
Fig. 5. Occurrences of air bubbles at the installation height $H = d$

(a)   (b)
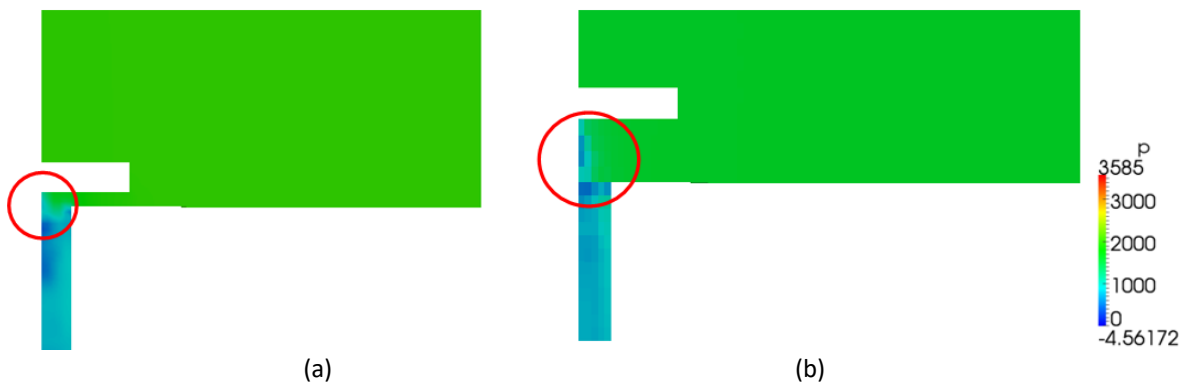
Fig. 6. Contrast of low-pressure areas at distinct installation heights (a) $H = 0.25d$ (b) $H = 1d$

3.1.1.3 Draining process under the influence of air bubbles and air-core vortex

The presence of air bubbles is likewise noted when the installation heights are raised to 2d, 3d, and 4d. Figure 7 illustrates the liquid fraction affected by either air bubbles or an air-core vortex. The findings indicate that the initiation of the air-bubble phenomenon typically occurs at t = 40 s, coinciding with the swirl velocity reaching the center of the tank. The formation of the air-core vortex, however, only takes place after the liquid surface has passed beyond the disc suppressor. These conditions are depicted in Figure 8.
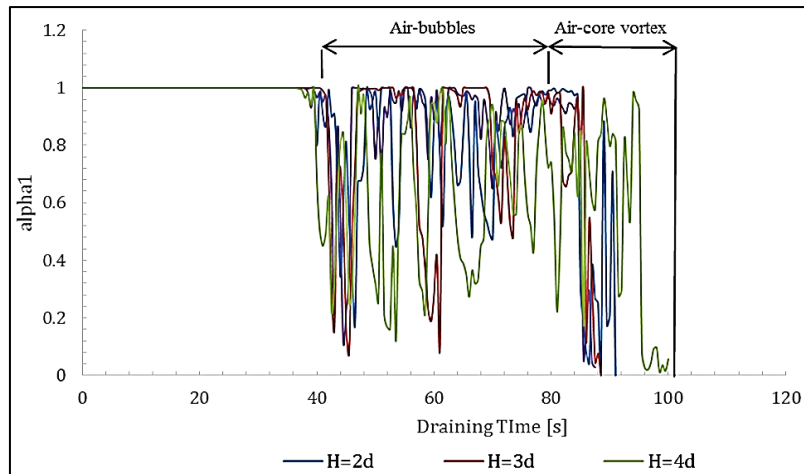
Fig. 7. Liquid fraction at the outlet for installation heights of $2d$, $3d$ and $4d$ during the air-core regime

(a) (b) (c)
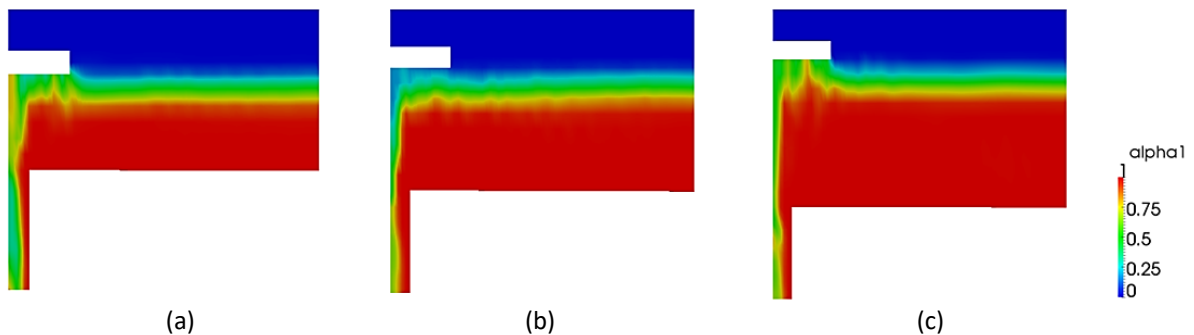
Fig. 8. Generation of the air-core vortex (a) $H = 2d$ (b) $H = 3d$ (c) $H = 4d$

3.1.2 Cone simulation

In the case of the disc, three distinct draining behavior regimes were identified. However, if the disc is substituted with a cone, only a single behavior is observed. The details of this process are elaborated in this section.

3.1.2.1 Draining process under the influence of air bubbles and air-core vortex

The drainage characteristics exhibit minimal changes when substituting the disc with cones of varying diameters (D_{cone}). For D_{cone} values of $2d$ and $3d$, as depicted in Figures 9(a) and 9(b), the liquid fraction at the outlet starts fluctuating once the liquid descends to a specific height $H = d$. If the cone diameter is further increased to $D_{cone} = 4d$, a more pronounced fluctuation in the liquid fraction is observed. These phenomena are attributed to the formation of air bubbles, as illustrated in Figure 10. As explained earlier, the introduction of a cone-shaped plate reduces the pressure near the outlet, allowing atmospheric air to be drawn into the tank's outlet. A smaller cone diameter results in a less significant low-pressure area, leading to fewer air bubbles being drawn into the tank, as shown in Figure 11 for comparison.
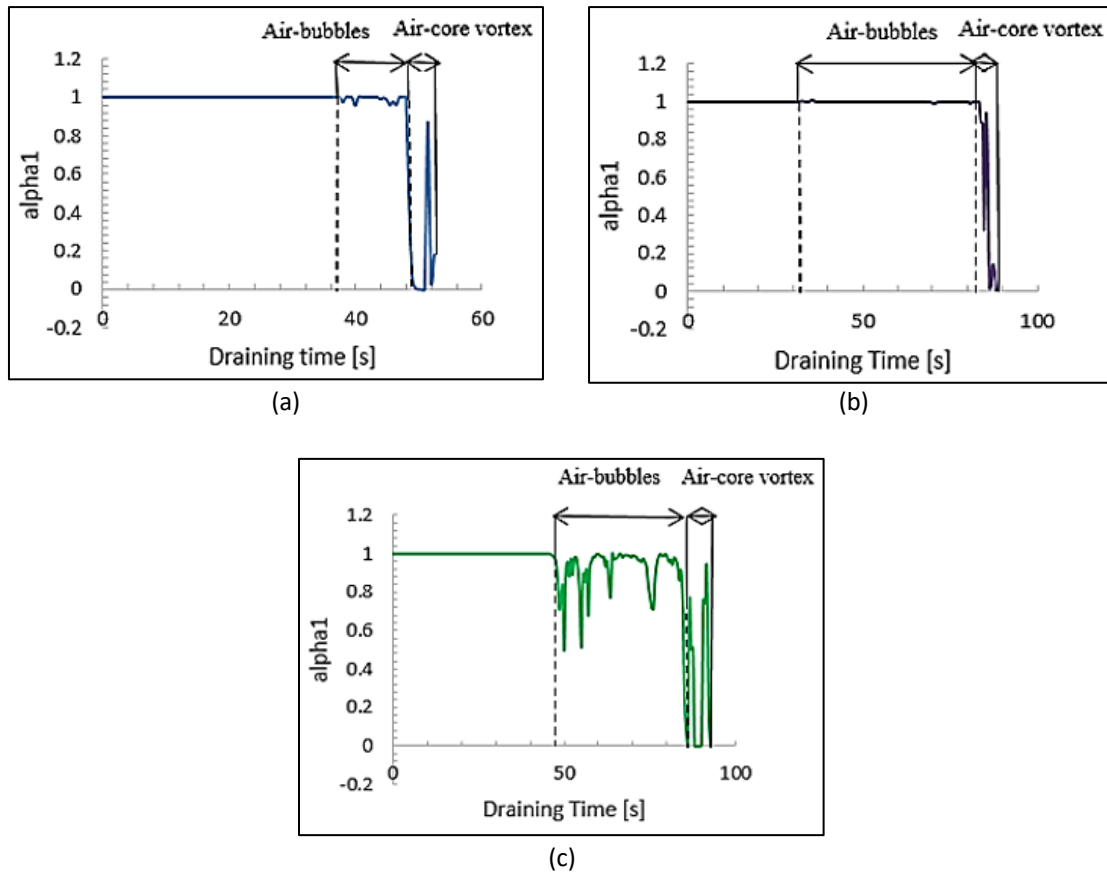
Fig. 9. Liquid fraction at the outlet for diameters during the air-core regime (a) 2d (b) 3d (c) 4d

Fig. 10. Air-bubble occurrence with $D_{cone} = 2d$
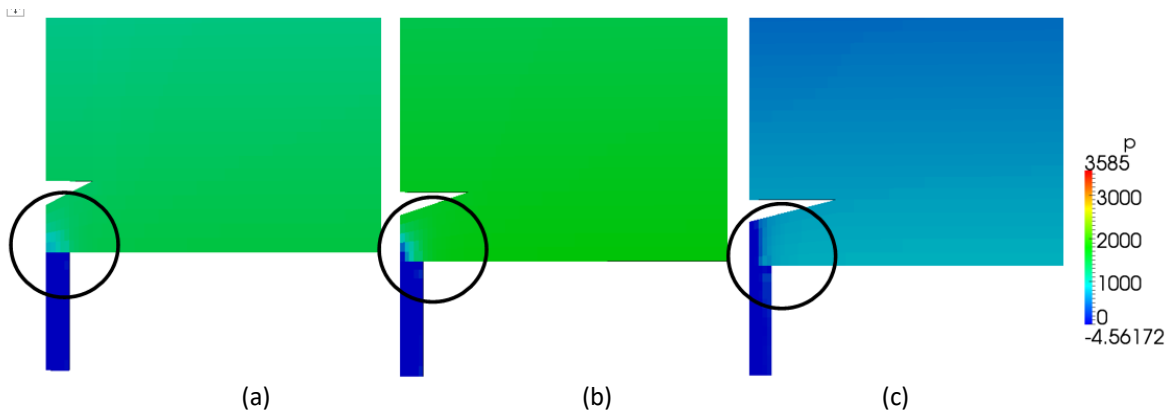
Fig. 11. Low-pressure areas for various diameters (a) $D_{cone} = 2d$ (b) $D_{cone} = 3d$ (c) $D_{cone} = 4d$

In the concluding stage of the drainage process, the liquid fraction experiences fluctuations. This fluctuation is induced by the air-core vortex, emerging just after the liquid passes the cone plate in each case (refer to Figures 12(a) to 12(c)). The air-core is drawn downward into the outlet and persists for 2 to 3 seconds before the completion of the drainage process.
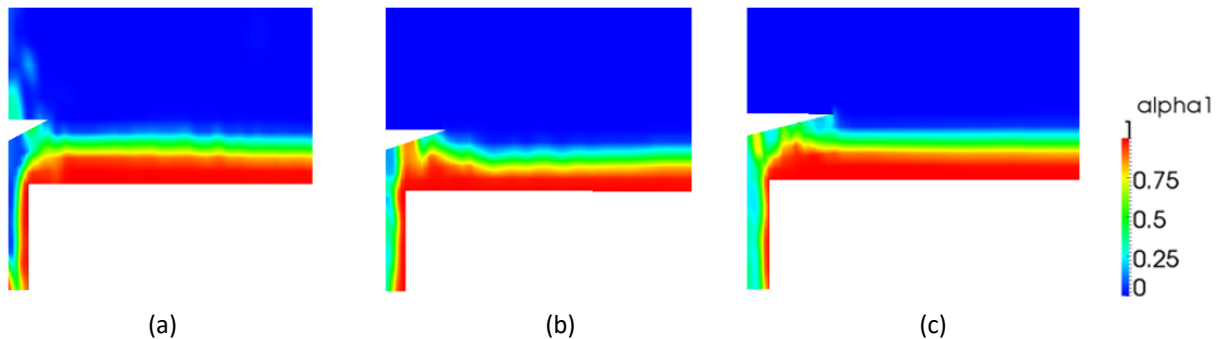
Fig. 12. Generation of the air-core vortex (a) D_cone=2d (b) D_cone=3d (c) D_cone=4d

3.2 Flow Visualisation

These Figures 13 to 16 provide comparative vector plots of streamline and instantaneous velocity for selected cases involving discs ($H = 0.25d$, $H = d$, $H = 4d$) and one case with a cone $D_{cone} = 2d$. The draining process exhibits three distinct regimes in this scenario: normal draining process (for $H = 0.25$), transition process (for $H = d$) and bubbly draining (for $H = 4d$ and $D_{cone} = 2d$). The visualizations reveal similar flow patterns for cases with $H = 0.25d$ (steady draining) and $H = d$ (transition), while slight differences are observed in cases with $H = 4d$ and $D_{cone} = 2d$ cases (bubbly draining).
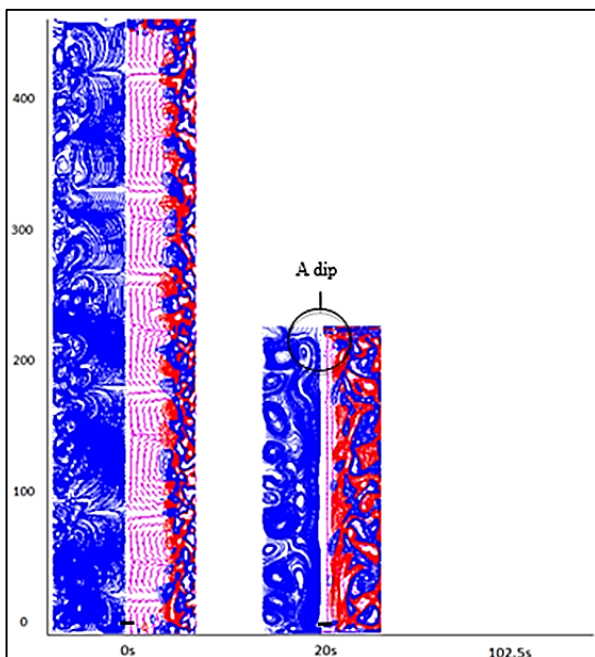
Fig. 13. Showcase streamline and instantaneous velocity vector plots (color-coded by vorticity strength) corresponding to the installation height of $H = 0.25d$ during the normal drainage regime
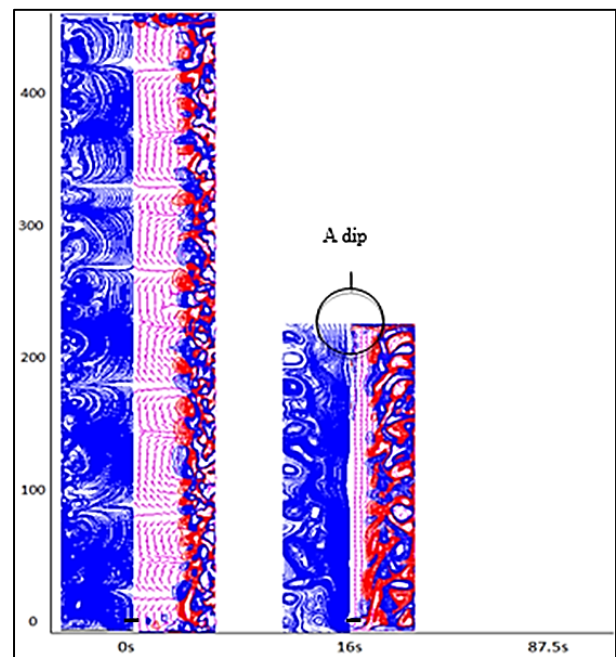
Fig. 14. Showcase streamline and instantaneous velocity vector plots (color-coded by vorticity strength) corresponding to the installation height of $H = d$ during the transition regime

At *t* = 0 s, due to the initial rotation, small vortices with high vorticity are observed near the tank wall, extending from the wall to approximately 25% of the tank radius. This condition forces liquid molecules into circular motion, generating irrotational flow at the tank center. Over time, the small vortices evolve into vortex rings, marking the onset of the second regime of behavior in the draining process. During this phase, the vortex rings strengthen and expand to nearly 60% of the tank radius from the wall. Consequently, a dip forms at *t* = 20 s (for *H* = 0.25*d*), *t* = 16 s (for *H* = *d*), *t* = 19.5 s (for *H* = 4*d*) or *t* = 15.5 s (for D_{cone} = 2*d*). As mentioned earlier, a dip is only observed for installation heights of $H = 0.25d$ and $H = d$, as the air-core vortex does not form in these cases. This dip persists until the liquid is completely drained but does not transform into an air-core.

A noteworthy flow pattern emerges in Figure 15 (at *t* = 80.5 s) and Figure 16 (at *t* = 49.5 s). At this moment, the air-core vortex forms immediately after the liquid passes the disc or cone plate. In Figure 15 (at *t* = 80.5 s), half of a vortex ring appears, while no vortex ring is observed in Figure 16 (at *t* = 49.5 s). This suggests that the formation of the air-core vortex is unaffected by Taylor vortices but is influenced by the critical height.
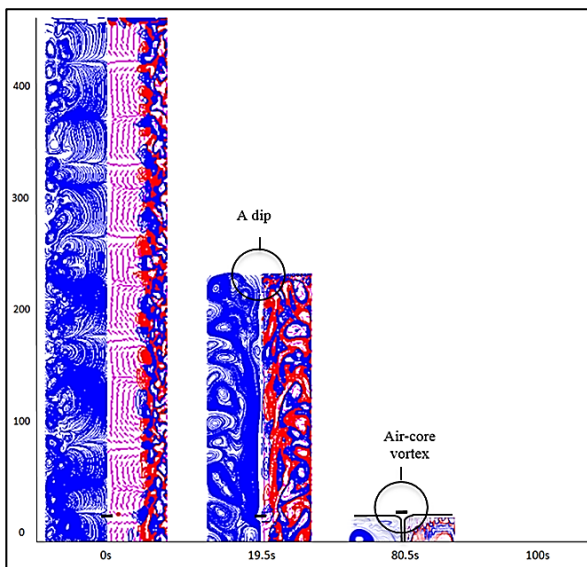
Fig. 15. Showcase streamline and instantaneous velocity vector plots (color-coded by vorticity strength) corresponding to the installation height of $H = 4d$ during the air-core regime
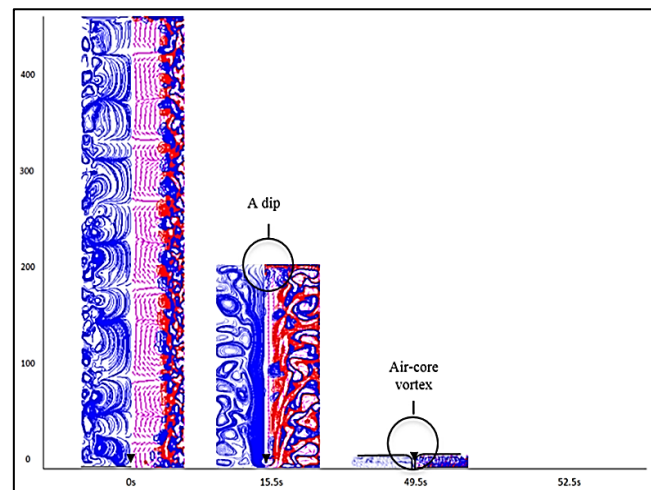
Fig. 16. Streamline and instantaneous velocity vector plots (color-coded by vorticity) for the diameter $D_{cone} = 2$ during the air-core regime

5. Conclusions

This research has advanced our comprehension on how a bluff-body can influence the emergence of an air-core vortex in a liquid-draining tank. Two bluff-body geometries, along with diverse installation conditions in simulations are examined. When a disc suppressor is in place, two distinct draining behaviors (the normal regime and air-core regime) separated by a transition regime are identified. A seamless draining process is observed if the bluff-body is installed below a specific height $H = d$.

The introduction of cones with varying diameters D_{cone} in place of the disc is significantly alter the drainage behavior. In the case of a cone plate, the draining process consistently results in the formation of an air-core vortex, albeit occurring later. For D_{cone} values of 2*d* and 3*d*, the liquid fraction at the outlet starts fluctuating once the liquid descends to a certain height $H = d$.

Acknowledgement

Reference

[1]   Trivellato, Filippo. "Anti-vortex devices: Laser measurements of the flow and functioning." *Optics and Lasers in Engineering* 48, no. 5 (2010): 589-599. https://doi.org/10.1016/j.optlaseng.2009.11.010

[2]   Basu, Prateep, Dheeraj Agarwal, T. John Tharakan, and Abdusamad Salih. "Numerical studies on air-core vortex formation during draining of liquids from tanks." *International Journal of Fluid Mechanics Research* 40, no. 1 (2013). https://doi.org/10.1615/InterJFluidMechRes.v40.i1.30

[3]   Sakri, Fadhilah Mohd, Mohamed Sukri Mat Ali, Sheikh Ahmad Zaki Shaikh Salim, and Sallehuddin Muhamad. "Numerical simulation of liquids draining from a tank using OpenFOAM." In *IOP Conference Series: Materials Science and Engineering*, 226, no. 1, p. 012152. IOP Publishing, 2017. https://doi.org/10.1088/1757-899X/226/1/012152

[4]   Sohn, Chang Hyun, Jong Hyeon Son, and Il Seouk Park. "Numerical analysis of vortex core phenomenon during draining from cylinder tank for various initial swirling speeds and various tank and drain port sizes." *Journal of Hydrodynamics, Ser. B* 25, no. 2 (2013): 183-195. https://doi.org/10.1016/S1001-6058(13)60353-4

[5]   Mathew, Sam, B. S. V. Patnaik, and T. John Tharakan. "Numerical study of air-core vortex dynamics during liquid draining from cylindrical tanks." *Fluid Dynamics Research* 46, no. 2 (2014): 025508. https://doi.org/10.1088/0169-5983/46/2/025508

[6]   McDuffie, Norton G. "Vortex free downflow in vertical drains." *AIChE Journal* 23, no. 1 (1977): 37-40. https://doi.org/10.1002/aic.690230107

[7]   Sinaga, Danieal Aderson, Muhamad Dwi Septiyanto, Zainal Arifin, Gunawan Rusdiyanto, Singgih Dwi Prasetyo, and Syamsul Hadi. "The effect of blade distances on the performance of double-stage gravitational water vortex turbine." *Journal of Advanced Research in Fluid Mechanics and Thermal Sciences* 109, no. 1 (2023): 196-209. https://doi.org/10.37934/arfmts.109.1.196209

[8]   Nazmy, Sikh Ilham, Zambri Harun, Zulkhairi Zainol Abidin, Mohd Izhar Ghazali, and Junaidy Ilyas. "Vortex Control Using Plate Type Floor Splitter in Pump Intake." *Journal of Advanced Research in Fluid Mechanics and Thermal Sciences* 100, no. 1 (2022): 89-97. https://doi.org/10.37934/arfmts.100.1.8997

[9]   Aziz, Muhammad Qamaran Abdul, Juferi Idris, and Muhammad Firdaus Abdullah. "Experimental study on enclosed gravitational water vortex turbine (GWVT) producing optimum power output for energy production." *Journal of Advanced Research in Fluid Mechanics and Thermal Sciences* 95, no. 2 (2022): 146-158. https://doi.org/10.37934/arfmts.95.2.146158

[10]   Gowda, B. H. L., S. Akhuli, B. R. Anudeep, K. R. Ipe, and K. Kishore. "Influence of base inclination on vortex formation during draining from cylindrical tanks." *Indian Journal of Engineering & Materials Sciences* 20, no. 5 (2013): 361-366.

[11]   Uki, Tamagna, Subhash T. Sarda, and Thomas Mathew. "Design of gas-liquid separator for complete degasing." *International Journal of Chemical Engineering and Applications* 3, no. 6 (2012): 477-480. https://doi.org/10.7763/IJCEA.2012.V3.247

[12]   Chu, In-Cheol, Chul-Hwa Song, Bong Hyun Cho, and Jong Kyun Park. "Development of passive flow controlling safety injection tank for APR1400." *Nuclear Engineering and Design* 238, no. 1 (2008): 200-206. https://doi.org/10.1016/j.nucengdes.2007.07.002

[13]   Sohn, Chang Hyun, Myoung Gun Ju, and BH Lakshmana Gowda. "Draining from cylindrical tanks with vane-type suppressors—A PIV Study." *Journal of Visualization* 12 (2009): 347-360. https://doi.org/10.1007/BF03181878

[14]   Mengali, Giovanni, and Alessandro A. Quarta. "Vane-type suppressor to prevent vortexing during draining from cylindrical tanks." *Journal of Spacecraft and Rockets* 42, no. 2 (2005): 381-383. https://doi.org/10.2514/1.8624

[15]   Uki, Tamagna, Subhash T. Sarda, and Thomas Mathew. "Design of gas-liquid separator for complete degasing." *International Journal of Chemical Engineering and Applications* 3, no. 6 (2012): 477-480. https://doi.org/10.7763/IJCEA.2012.V3.247

[16]   Mahyari, Mahdi N., Hasan Karimi, Hasan Naseh, and Mehran Mirshams. "Numerical and experimental investigation of vortex breaker effectiveness on the improvement in launch vehicle ballistic parameters." *Journal of Mechanical Science and Technology* 24 (2010): 1997-2006. https://doi.org/10.1007/s12206-010-0618-7

[17] Abramson, H. Norman, Wen-Hwa Chu, and Luis R. Garza. *Some studies of liquid rotation and vortexing in rocket propellant tanks*. National Aeronautics and Space Administration, 1962.

[18] Kinefuchi, Kiyoshi, Toru Kamita, Hideyo Negishi, Keisuke Yamada, and Masanobu Fujimura. "Experimental and numerical simulation study of liquid-propellant draining from rocket tanks." *Journal of Spacecraft and Rockets* 47, no. 5 (2010): 860-864. https://doi.org/10.2514/1.48398

[19] Sohn, Chang Hyun, Myoung Gun Ju, and BH Lakshmana Gowda. "Draining from cylindrical tanks with vane-type suppressors—A PIV Study." *Journal of Visualization* 12 (2009): 347-360. https://doi.org/10.1007/BF03181878

[20] Sohn, Chang-Hyun, B. H. L. Gowda, and Myoung-Gun Ju. "Eccentric drain port to prevent vortexing during draining from cylindrical tanks." *Journal of Spacecraft and Rockets* 45, no. 3 (2008): 638-640. https://doi.org/10.2514/1.35651

[21] Sohn, C. H., M. G. Ju, and B. H. L. Gowda. "PIV study of vortexing during draining from square tanks." *Journal of Mechanical Science and Technology* 24 (2010): 951-960. https://doi.org/10.1007/s12206-010-0207-9

[22] Jasak, Hrvoje. "Error analysis and estimation in the Finite Volume method with applications to fluid flows." (1996).

[23] Versteeg, Henk Kaarle. *An introduction to computational fluid dynamics the finite volume method, 2/E*. Pearson Education India, 2007.

[24] Aris, Rutherford. *Vectors, tensors and the basic equations of fluid mechanics*. Courier Corporation, 2012.

[25] Jiang, Xi, and Choi-Hong Lai. *Numerical techniques for direct and large-eddy simulations*. CRC press, 2016. https://doi.org/10.1201/9781420075793